Nano Res. 2011, 4(10): 996–1004
DOI 10.1007/s12274-011-0156-3
Research Article

ISSN 1998-0124
CN 11-5974/O4

The Origin of Wrinkles on Transferred Graphene

Nan Liu[§], Zhonghuai Pan[§], Lei Fu[§], Chaohua Zhang, Boya Dai, and Zhongfan Liu (✉)

Center for Nanochemistry (CNC), Beijing National Laboratory for Molecular Sciences, State Key Laboratory for Structural Chemistry of Unstable and Stable Species, College of Chemistry and Molecular Engineering, Academy for Advanced Interdisciplinary Studies, Peking University, Beijing 100871, China

[§] These authors contributed equally to this work.

Received: 30 April 2011 / Revised: 26 May 2011 / Accepted: 1 June 2011

ABSTRACT

When two-dimensional graphene is exfoliated from three-dimensional highly oriented pyrolytic graphite (HOPG), ripples or corrugations always exist due to the intrinsic thermal fluctuations. Surface-grown graphenes also exhibit wrinkles, which are larger in dimension and are thought to be caused by the difference in thermal expansion coefficients between graphene and the underlying substrate in the cooling process after high temperature growth. For further characterization and applications, it is necessary to transfer the surface-grown graphenes onto dielectric substrates, and other wrinkles are generated during this process. Here, we focus on the wrinkles of transferred graphene and demonstrate that the surface morphology of the growth substrate is the origin of the new wrinkles which arise in the surface-to-surface transfer process; we call these morphology-induced wrinkles. Based on a careful statistical analysis of thousands of atomic force microscopy (AFM) topographic data, we have concluded that these wrinkles on transferred few-layer graphene (typically 1–3 layers) are determined by both the growth substrate morphology and the transfer process. Depending on the transfer medium and conditions, most of the wrinkles can be either released or preserved. Our work suggests a new route for graphene engineering involving structuring the growth substrate and tailoring the transfer process.

KEYWORDS

Graphene, wrinkle, transfer, surface topography, atomic force microscopy

1. Introduction

Strictly two-dimensional (2D) crystals are thermodynamically unstable [1]. Crumpling in the third dimension of mono- or few-layer graphene leads to an increase in elastic energy but minimizes the total free energy which enables the existence of graphene [2, 3]. Ripples on mechanically exfoliated graphene, with ~1-nm-high corrugations and 10–25-nm-lateral dimensions, have been invoked to explain many phenomena [4], such as decreased carrier mobility [5], suppression of weak localization [6], formation of electron–hole puddles [7], and enhanced chemical reactivity [8]. As a low cost and scalable technique for obtaining large-area, high-quality, and uniform graphene films, surface growth methods represented by chemical vapor deposition (CVD) have recently attracted great attention [9–11]. When employing these surface-grown graphenes in fundamental research or practical applications, a transfer procedure from the

Address correspondence to zfliu@pku.edu.cn

metal substrates to dielectric substrates is a prerequisite [12]. Wrinkles always appear on these transferred surface-grown graphenes [10, 11, 13]. Typically, the corrugation of these wrinkles is ~2–15 nm in height, and ~20–100 nm in width (see in the Electronic Supplementary Material (ESM), Figs. S-1, S-2 and Tables S-1, S-2), larger than the ripples on mechanically exfoliated graphene, which strongly influences the physicochemical properties of the graphene sample [14].

The origin of wrinkles on transferred surface-grown graphene is not yet fully understood. The wrinkles are usually considered to be a result of compressive stress during cooling caused by the difference in thermal expansion coefficients between graphene and metals [15]. Here, we focus on this fundamental issue for transferred few-layer graphene. We found that with the widely-used surface-to-surface transfer technique [16], there is a strong correlation between the surface morphology of the growth substrate and wrinkle distribution, and the transfer process also plays an important role in determining the final wrinkle density of the transferred graphene.

2. Experimental

2.1 Growth of few-layer graphene films

To study the mechanisms of wrinkle formation on transferred graphene, three kinds of few-layer graphene were prepared. The segregation growth of graphene was carried out on evaporated Ni films, which were deposited on thermally oxidized silicon wafers by ultra-high vacuum (UHV) electron beam deposition (ULS400, Balzers). The Ni target was commercially available (General Research Institute for Nonferrous Metals, China) with a Ni purity of > 99.9 wt.% and the evaporated Ni film had a carbon content of ~2.6 at.% in the bulk as determined by X-ray photoelectron spectroscopy (XPS). The typical thickness of the polycrystalline Ni films was 150–500 nm. Thus-prepared Ni films were placed in a vacuum annealing furnace (VTHK-350, Beijing Technol Science Co., Ltd.) at 1100 ℃ and 4×10^{-3} Pa for graphene growth. The layer distribution of graphene was as high as ~82% for 1–3 layers, confirmed by optical contrast and Raman spectroscopy (see Table S-3 and Fig. S-3 in the ESM). The CVD growth of graphene was conducted on either Ni films or Cu foils. The Ni-based-CVD was carried out on the same evaporated Ni film at 1000 ℃ and atmospheric pressure with a slow cooling speed (4 ℃/min), and by controlling the carbon precipitation resulted in graphene composed mostly of 1–3 layers. The Cu-based CVD was carried out on 25-μm-thick Cu foils (Alfa Aesar) in a thermal tube furnace at 1000 ℃ and 60 Pa (2 standard cubic centimeters per minute (sccm) H_2 and 35 sccm of CH_4 flow) and the resulting graphene existed mainly as monolayers.

2.2 Transfer process

All the surface-grown graphene films were transferred from metal substrates to 300 nm-SiO_2/Si substrates by the widely-used transfer technique [16]. The typical procedure includes: (1) spin-coating poly(methyl methacrylate) (PMMA, MicroChem AR-P 679.04, 950,000 MW, 4 wt.% in ethyl lactate) solution onto the graphene-on-metal substrates at 2000 r/min and baking the sample at 170 ℃ to completely remove the solvent and ensure the graphene became thoroughly embedded in the polymer; (2) releasing the flexible PMMA/graphene film in dilute HCl (1:1 vol.) or $FeCl_3$ (~1 mol/L) aqueous solution by etching off the underlying metal and attaching the PMMA/graphene film onto the target substrate; and (3) lifting off the PMMA by dissolving it in acetone.

2.3 Characterization

Atomic force microscopy (AFM, Veeco Instruments, Nanoscope IIIA) was used for the topographic imaging. All the AFM images were captured in 512 × 512 pixels by a standard silicon nitride probe (Model NP), typically with a cantilever of 100 μm in length and tens of nm in diameter at the apex.

Scanning electron microscopy (SEM, Hitachi-S4800) was also carried out to examine the effect of the surface-transfer process on wrinkle formation. All the SEM images were taken directly using a high voltage of 1 kV.

3. Results and discussion

Figure 1(a) shows a typical AFM image of 200 nm-thick vacuum-evaporated Ni film on a SiO_2/Si substrate

after segregation growth of graphene at 1100 ˚C and 4×10^{-3} Pa [13], which has the characteristic atomic flat crystal terraces, step edges and deep trenches. Shown in Fig. 1(b) is the corresponding AFM image of the transferred graphene film on a 300 nm-SiO_2/Si substrate obtained by utilizing a standard transfer technique with PMMA film [16]. It is obvious that there is a strong topographic correlation between two AFM images. The transferred graphene film has many wrinkles, resembling the original Ni film after high-temperature annealing treatment. When focusing on a specific Ni grain on the growth substrate, one can occasionally find isolated line-shaped wrinkles (Fig. 1(c)), which are believed to arise from the difference between the thermal expansion coefficients of graphene and Ni [15]. Similar line-shaped wrinkles can also be observed on the transferred graphene (Fig. 1(d)), although it is difficult to make a direct correlation between the growth substrate and the transferred samples. The wrinkles on transferred graphene can be roughly classified into three geometric types. The first type is a closed wrinkle encompassing an isolated area (encircled by white dots in Fig. 1(b)), which most probably corresponds to an isolated Ni grain on the growth substrate (encircled by white dots in Fig. 1(a)). Line-scan height profiles of an individual Ni grain and a closed wrinkle are shown in the insets of Figs. 1(a) and 1(b). The second type is a bi-wrinkle featuring two parallel lines in close proximity (traced by two dotted lines in the bottom part of Fig. 1(b)), which is

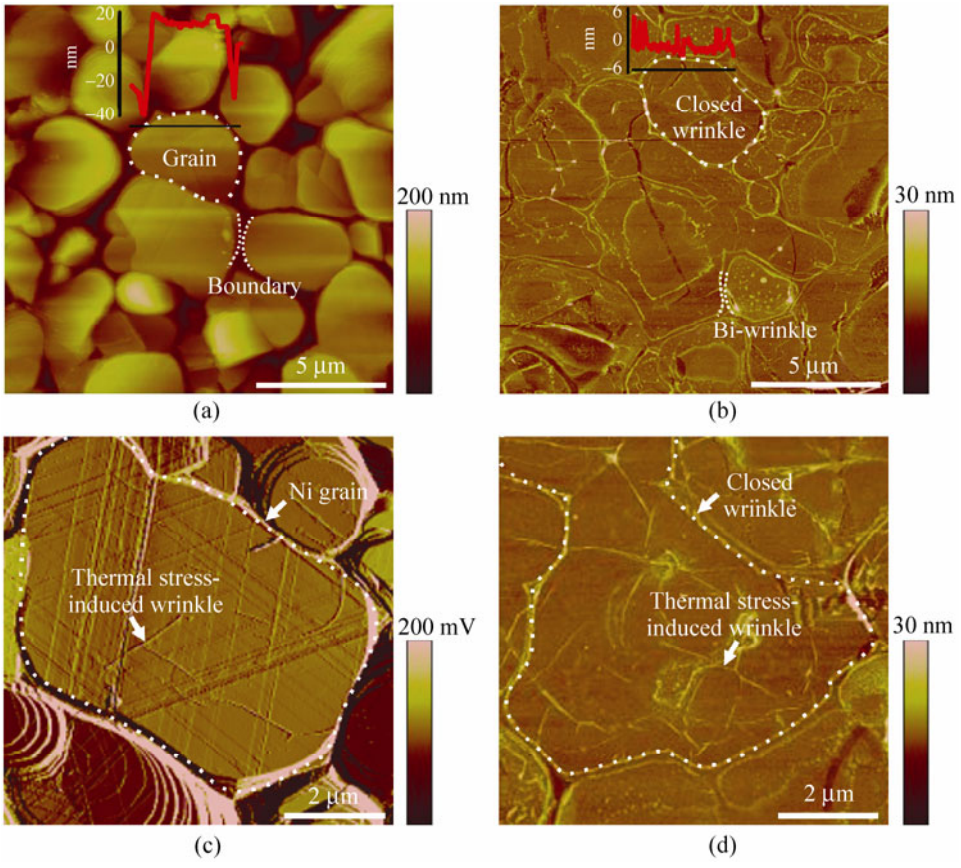

Figure 1 (a) AFM image of 200 nm-Ni film on a 300 nm-SiO_2/Si substrate after segregation growth of graphene at 1100 ˚C and 4×10^{-3} Pa, in which the dotted circle refers to an isolated Ni grain while two adjacent dotted lines correspond to a boundary formed between two Ni grains. The height profile of the black line is shown in the inset. (b) AFM image of transferred graphene film on a 300 nm-SiO_2/Si substrate using a PMMA transfer medium, in which the dotted circle and the two adjacent dotted lines highlight the closed wrinkle and bi-wrinkle, respectively. The height profile of the black line is shown in the inset. (c) Amplitude mode AFM image focusing on a specific Ni grain on the growth substrate, which shows the thermal stress-induced wrinkle. (d) Magnified AFM image of transferred graphene on a SiO_2/Si substrate showing the existence of wrinkles within a closed wrinkle

believed to arise from the deep boundary area between two adjacent Ni grains on the growth substrate (traced by two dotted lines in Fig. 1(a)). The third type is an isolated line-shaped wrinkle originating from the thermal stress effect as mentioned above; these are randomly distributed and have smaller sizes (see Fig. S-4 in the ESM).

In order to confirm whether the closed wrinkles and bi-wrinkles arose from the Ni grains and the inter-grain boundaries, respectively, we performed a statistical analysis of > 1000 AFM topographic data over an area of 10,000 μm^2 on the growth substrate and transferred graphene. Figure 2(a) shows the area distributions of isolated Ni grains on the growth substrate and closed wrinkles on the transferred graphene. The corresponding statistical data are listed in Table 1.

The Pearson correlation coefficient obtained from the statistical data is 0.95, suggesting the strong dependence of the closed graphene wrinkles on the original Ni grains of growth substrate. Similarly, we made a statistical analysis of the boundary widths formed between adjacent Ni grains and the bi-wrinkle widths on transferred graphene over using 400 data as shown in Fig. 2(b) and Table 2. Their close similarity with a Pearson correlation coefficient of ~0.99 indicates that there is a strong correlation between the Ni inter-grain boundaries and bi-wrinkle formation. From the above statistical analyses, we may draw a preliminary representation of the surface morphology-related wrinkle formation on transferred graphene as schematically illustrated in Fig. 2(c). On the Ni substrate, the whole surface was covered by graphene

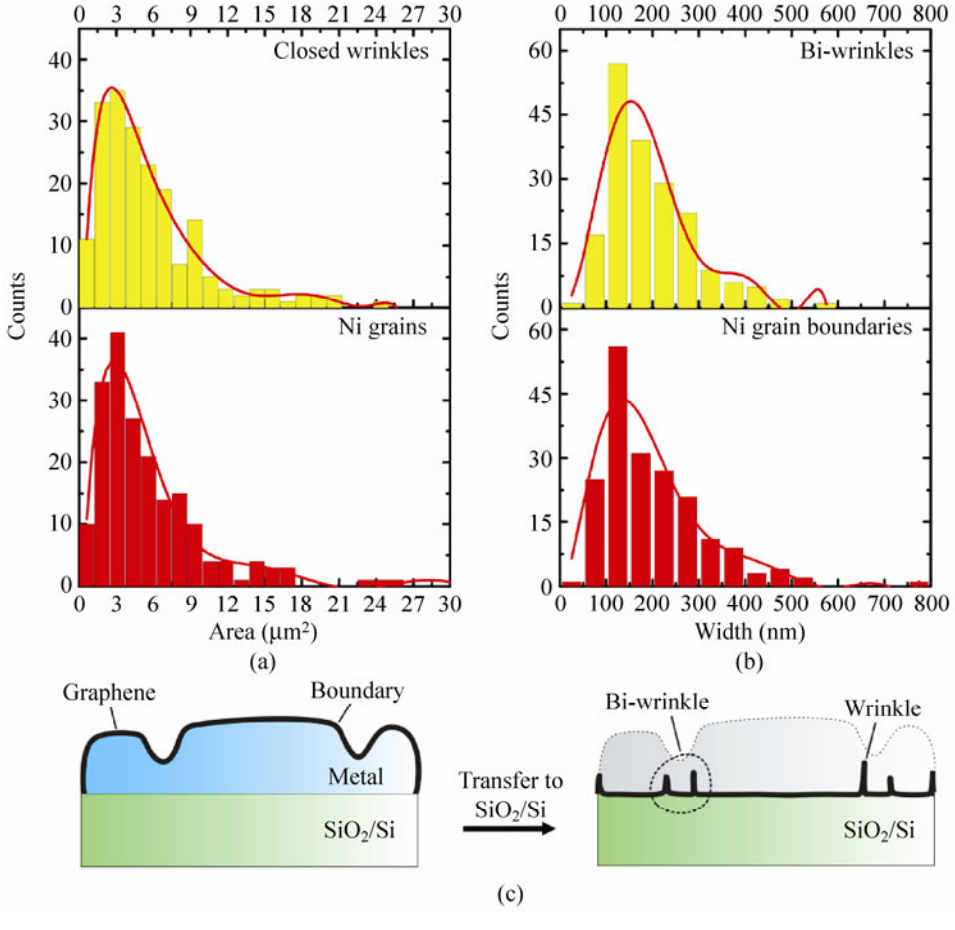

Figure 2 (a) Histograms of area distributions of Ni grains on the growth substrate (bottom) and closed wrinkles on transferred graphene (top), respectively. (b) Distributions of boundary widths formed between two adjacent Ni grains (bottom) and the bi-wrinkle widths (top), respectively. The red curves in the histograms are the polynomial fitting. (c) Schematic illustration of the surface-topography-preserved transfer process of graphene from a corrugated metal substrate to a smooth SiO_2/Si substrate

Table 1 Statistical data for Ni grains and closed wrinkle areas

	Mean area (μm^2)	Standard deviation (μm^2)	Pearson correlation coefficient
Ni grain	5.15	4.82	0.95
Closed wrinkle	5.53	4.33	

Table 2 Statistical data for Ni grain boundaries and bi-wrinkle widths

	Mean width (nm)	Standard deviation (nm)	Pearson correlation coefficient
Ni grain boundary	193.99	109.94	0.99
Bi-wrinkle	189.48	96.37	

after high-temperature annealing, as evidenced by the excellent continuity of the transferred graphene film. In a standard transfer process, the highly-flowing PMMA transfer medium replicates most of the topographic features of the Ni film. After transfer-printing onto the smooth SiO_2/Si substrate and removing the PMMA film, these replicated topographic features may not be completely released because of the extra graphene area and the pinning effect from the SiO_2/Si substrate [17]. As a result, the typical structural features of growth substrate are preserved on the transferred graphene film.

Direct evidence of growth surface morphology-induced wrinkle formation is shown in Fig. 3, where the graphene films were CVD-grown on Ni/SiO_2/Si substrates with different thicknesses of catalytic Ni films [18]. The sizes of Ni grains gradually decreased with the increase of Ni film thickness after high-temperature graphene growth (Figs. 3(a)–3(c)). The wrinkles on the transferred graphene films clearly exhibit a similar trend, with smaller Ni grains resulting in smaller closed wrinkles, and vice versa (Figs. 3(d)–3(f)). The 500 nm-Ni film leads to the highest density of wrinkles. In other words, the wrinkle density for CVD graphene can be regulated by the surface morphology of the Ni film. Under atmospheric growth conditions, the grain boundaries formed on the Ni film are relatively shallow compared with those at low growth pressure [19], which well explains the decrease in the number of the closed wrinkles considering the possible loss of shallow wrinkles during the transfer process. As an indicator of wrinkle density, we measured the total length of wrinkles on transferred graphene per μm^2, and plotted the value against Ni film thickness. The detailed method for measuring the length density of wrinkles on transferred graphene using "Image-Pro Plus" software is described in the ESM (see Fig. S-5). Figure 3(g) gives the statistics over an area of 4000 μm^2 together with Ni grain size. There is a clear correlation between wrinkle density and Ni grain size, strongly suggesting that the surface morphology of the metal substrate greatly contributes to the wrinkle formation on transferred graphene.

Vacuum-evaporated thin Ni films on SiO_2/Si substrates tend to form submicrometer to micrometer sized grains after thermal annealing treatment, with the grain size being strongly affected by the wettability of Ni on the SiO_2 surface [20]. This is partly responsible for the high density of wrinkles on transferred graphene. Cu foils have recently been frequently employed as CVD growth substrates for graphene, since they generate large-area and high-uniform monolayer graphene under low pressure due to the limited carbon solubility and self-limiting effect [11, 21]. Figure 4(a) shows the amplitude mode AFM image of Cu foil after CVD growth of graphene at 1000 °C. Instead of micrograins, we observed a large number of shallow parallel lines in this case, which originate from the mechanical processing of the Cu foil [22]. Large atomic flat terraces are overlapped with these mechanically-induced parallel lines. It is not difficult to discriminate the thermal stress-induced wrinkles from the parallel lines on such a Cu foil substrate featuring a random distribution and large dimensions (see Fig. S-6 in the ESM). Figure 4(b) shows the AFM image of CVD-graphene grown on Cu foil after transfer to a 300 nm-SiO_2/Si substrate using the standard transfer technique with a commercial PMMA solution as described in the Experimental (MicroChem AR-P 679.04, 950,000 MW, 4 wt.% in ethyl lactate) [16]. The morphology of the transferred graphene retains the topographic features of the original Cu foil, with many parallel wrinkles on the graphene surface. The distances between parallel wrinkles and Cu line steps are quite consistent, with a value of ~200 nm. This similarity suggests that the parallel wrinkles arise from the mechanically-induced line structures of Cu

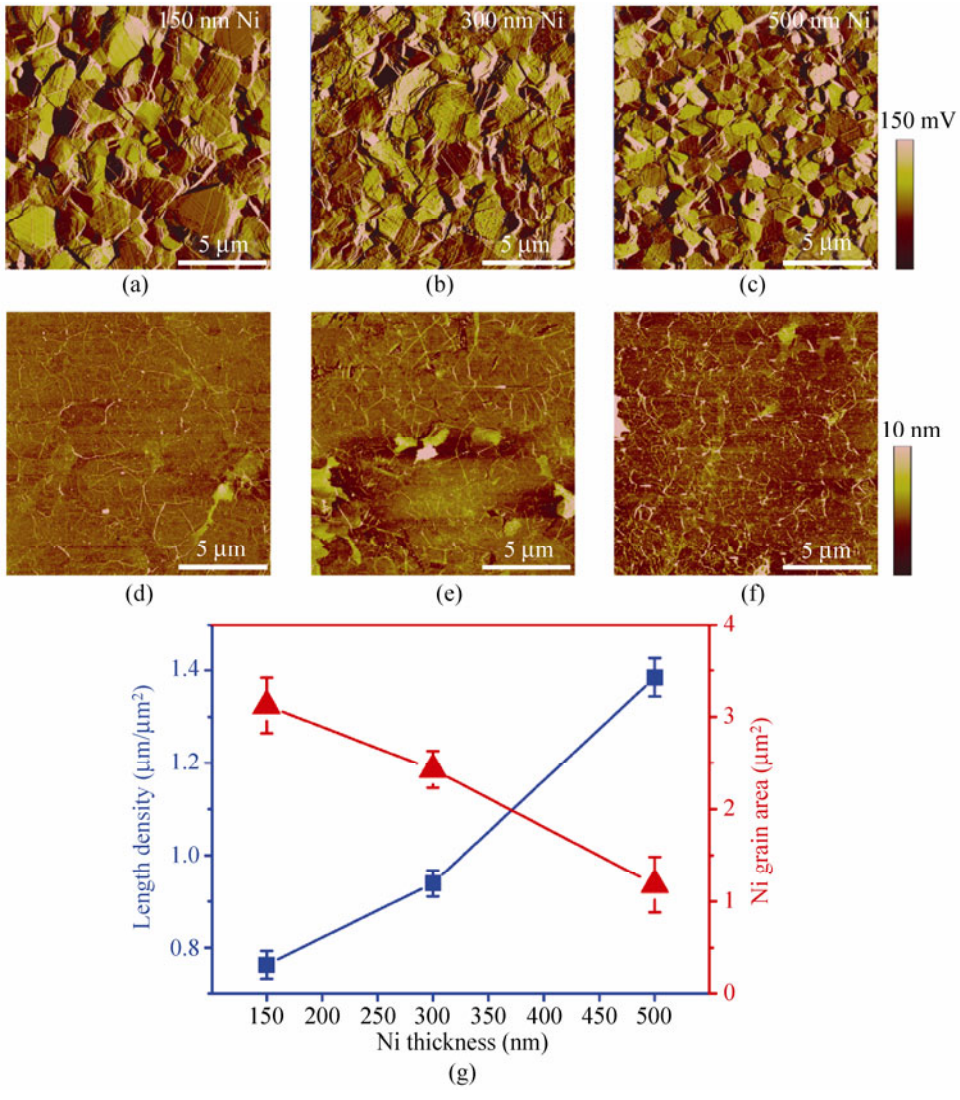

Figure 3 (a)–(c) Amplitude mode AFM images of 150, 300, and 500 nm Ni films after CVD growth of graphene at 1000 ˚C and atmospheric pressure. (d)–(f) Height mode AFM images of transferred graphene on 300 nm-SiO_2/Si substrates corresponding to (a)–(c). (g) Dependence of wrinkle density and Ni grain size on Ni film thickness

foil. However, by using our homemade PMMA solution having a larger molecular mass (Sigma–Aldrich solid product, ~996,000 MW, dissolved in ethyl lactate with a concentration of 4 wt.%), these wrinkles are almost completely released as seen in Fig. 4(c). Larger non-parallel wrinkles remain and may originate from thermal stress induction. These observations for the Cu foil system clearly indicate that the growth–substrate morphology-induced wrinkles can be either retained or released, depending on the transfer medium used in the transfer process.

To examine the effect of the surface-to-surface transfer process on wrinkle formation, we followed all the transfer steps of the widely-used standard transfer process as shown in Figs. 5(a)–5(d) [16]. As mentioned above, the Ni film after segregation growth of graphene at 1100 ˚C and 4×10^{-3} Pa is characterized by submicrometer- to micrometer-sized grains (Fig. 5(a)). After spin-coating with a ~200 nm PMMA film (MicroChem AR-P 679.04, 950,000 MW, 4 wt. % in ethyl lactate, 2,000 r/min), these micrograins are completely covered and embedded by the polymer (Fig. 5(b)). By

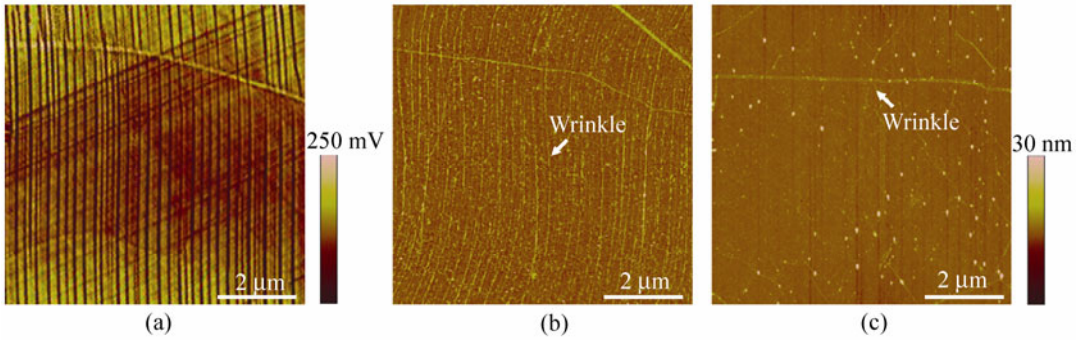

Figure 4 (a) Amplitude mode AFM image of Cu foil after CVD growth of graphene at 1000 ˚C and a low pressure of 60 Pa. (b) and (c) AFM images of the corresponding graphene with preserved and released topographic features of Cu foils, transferred onto 300 nm-SiO_2/Si substrates using a PMMA film made from a commercial solution (MicroChem AR-P 679.04, 950,000 MW, 4 wt.% in ethyl lactate) and from a homemade solution (Sigma–Aldrich solid product, ~996,000 MW, dissolved in ethyl lactate with a concentration of 4 wt.%), respectively

etching off the Ni layer with dilute hydrochloric acid and partly removing the PMMA layer with acetone, some of the original micrograin structures disappeared as seen in Fig. 5(c). After completely removing the PMMA layer on a 300 nm-SiO_2/Si substrate, similar micrograin features are visible again (Fig. 5(d)). These observations clearly suggest that at least some of the topographic features of the growth substrate have been preserved on transferred graphene obtained using the standard transfer technique.

Figure 6 reveals the effect of the transfer conditions on wrinkle formation. Simply by soaking the PMMA/graphene film in deionized water, we can drastically reduce the density of wrinkles on transferred graphene (see Figs. 6(a) and 6(b)). The wrinkle density gradually decreases with increasing soaking time, as seen in Fig. 6(c). We believe that the large surface tension of water flattens the wrinkles preserved by the PMMA transfer medium. Over 70% of wrinkles were removed after soaking in water for 30 min. As a consequence, the details of the surface transfer technique, including the transfer medium and the experimental conditions strongly affect the wrinkle formation on transferred graphene.

Finally, it should be pointed out that as mentioned by Obraztsov et al. [15], formation of wrinkles is also related to the thickness of the graphene film. Actually, we did observe a change in wrinkle distribution on thick CVD graphene (> 10 layers) on a Ni substrate (see Fig. S-7 in the ESM). Such wrinkles mostly arise from the thermal stress effect and are clearly visible even on a rough Ni surface because of the increase in wrinkle height [23, 24].

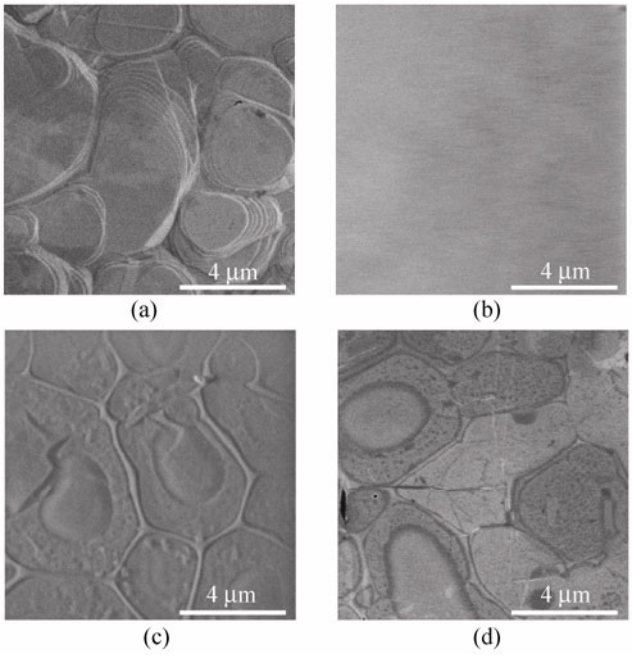

Figure 5 SEM images monitoring each step of the transfer process of graphene from the growth to target substrates. (a) 200 nm-Ni film on SiO_2/Si after segregating graphene at 1100 ˚C and 4 × 10^{-3} Pa. (b) After spin-coating a ~200 nm PMMA layer on the sample (a). (c) After etching off the Ni layer in dilute hydrochloric acid and partly removing the PMMA layer with acetone. (d) After completely removing the PMMA layer on the 300 nm-SiO_2/Si substrate

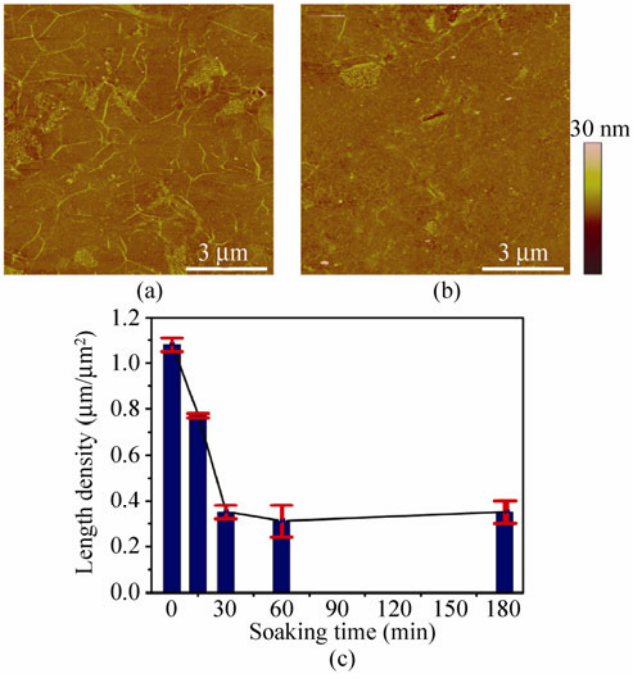

Figure 6 Effect of experimental transfer conditions on wrinkle formation. (a) and (b) AFM images of transferred graphene on 300 nm-SiO_2/Si substrates after soaking in water for 1 min and 60 min, respectively. (c) Dependence of wrinkle density on soaking time in deionized water. All the graphene samples were grown from evaporated 200 nm-Ni films using atmospheric CVD

4. Conclusions

The wrinkles of 2D graphene have rather complicated origins. In addition to the well-accepted model based on the difference between the thermal expansion coefficients of graphene and the growth substrate, the morphology of the growth substrate may also significantly contribute to the wrinkle formation, depending on the transfer technique employed for transferring graphene from the growth to target substrates. Depending on the transfer medium and the details of the experimental conditions, the wrinkles can be either released or preserved on few-layer graphene. Our work suggests a new route for engineering 2D graphene. We may tune the physicochemical properties of graphene by modulating the density and even the structures of wrinkles by structural design of the growth substrate. Such wrinkle engineering of 2D graphene is under way in our laboratory.

Acknowledgements

The research was supported by the Natural Science Foundation of China (Grants Nos. 51072004, 50802003, 20973013, and 50821061) and the Ministry of Science and Technology of China (Grants Nos. 2007CB936203, 2009CB29403, 2011CB933003, and 2011CB921903).

Electronic Supplementary Material: Further details and discussions of the wrinkle dimension of transferred graphene, determination of the layer number of transferred graphene, the size differences between two kinds of wrinkles on transferred graphene, the method for measuring the length density of wrinkles on transferred graphene, the thermal stress-induced wrinkles on Cu foil after thermal annealing, and the wrinkle distribution on thick graphene are available in the online version of this article at http://dx.doi.org/10.1007/s12274-011-0156-3 and are accessible free of charge.

References

[1] Landau, L.; Lifshits, E.; Pitaevskii, L. *Statistical Physics, Part I*; Pergamon: Oxford, 1980.

[2] Novoselov, K. S.; Geim, A. K.; Morozov, S. V.; Jiang, D.; Zhang, Y.; Dubonos, S. V.; Grigorieva, I. V.; Firsov, A. A. Electric field effect in atomically thin carbon films. *Science* **2004**, *306*, 666–669.

[3] Geim, A.; Novoselov, K. The rise of graphene. *Nat. Mater.* **2007**, *6*, 183–191.

[4] Lui, C. H.; Liu, L.; Mak, K. F.; Flynn, G. W.; Heinz, T. F. Ultraflat graphene. *Nature* **2009**, *462*, 339–341.

[5] Katsnelson, M.; Geim, A. Electron scattering on microscopic corrugations in graphene. *Phil. Trans. R. Soc. A* **2008**, *366*, 195–204.

[6] Morozov, S. V.; Novoselov, K. S.; Katsnelson, M. I.; Schedin, F.; Ponomarenko, L. A.; Jiang, D.; Geim, A. K. Strong suppression of weak localization in graphene. *Phys. Rev. Lett.* **2006**, *97*, 016801.

[7] Martin, J.; Akerman, N.; Ulbricht, G.; Lohmann, T.; Smet, J. H.; Von Klitzing, K.; Yacoby, A. Observation of electron–hole puddles in graphene using a scanning single-electron transistor. *Nat. Phys.* **2008**, *4*, 144–148.

[8] Elias, D.; Nair, R.; Mohiuddin, T.; Morozov, S.; Blake, P.; Halsall, M.; Ferrari, A.; Boukhvalov, D.; Katsnelson, M.; Geim, A. Control of graphene's properties by reversible

hydrogenation: Evidence for graphane. *Science* **2009**, *323*, 610–613.

[9] Kim, K.; Zhao, Y.; Jang, H.; Lee, S.; Kim, J.; Ahn, J.; Kim, P.; Choi, J.; Hong, B. Large-scale pattern growth of graphene films for stretchable transparent electrodes. *Nature* **2009**, *457*, 706–710.

[10] Reina, A.; Jia, X.; Ho, J.; Nezich, D.; Son, H.; Bulovic, V.; Dresselhaus, M.; Kong, J. Large area, few-layer graphene films on arbitrary substrates by chemical vapor deposition. *Nano Lett.* **2009**, *9*, 30–35.

[11] Li, X. S.; Cai, W. W.; An, J. H.; Kim, S.; Nah, J.; Yang, D. X.; Piner, R.; Velamakanni, A.; Jung, I.; Tutuc, E.; Banerjee, S. K.; Colombo, L.; Ruoff, R. S. Large-area synthesis of high-quality and uniform graphene films on copper foils. *Science* **2009**, *324*, 1312–1314.

[12] Geim, A. Graphene: Status and prospects. *Science* **2009**, *324*, 1530–1534.

[13] Liu, N.; Fu, L.; Dai, B.; Yan, K.; Liu, X.; Zhao, R.; Zhang, Y.; Liu, Z. Universal segregation growth approach to wafer-size graphene from non-noble metals. *Nano Lett.* **2011**, *11*, 297–303.

[14] Guinea, F.; Katsnelson, M. I.; Vozmediano, M. A. H. Midgap states and charge inhomogeneities in corrugated graphene. *Phys. Rev. B* **2008**, *77*, 075422.

[15] Obraztsov, A.; Obraztsova, E.; Tyurnina, A.; Zolotukhin, A. Chemical vapor deposition of thin graphite films of nanometer thickness. *Carbon* **2007**, *45*, 2017–2021.

[16] Reina, A.; Son, H. B.; Jiao, L. Y.; Fan, B.; Dresselhaus, M. S.; Liu, Z. F.; Kong, J. Transferring and identification of single- and few-layer graphene on arbitrary substrates. *J. Phys. Chem. C* **2008**, *112*, 17741–17744.

[17] Liang, X.; Fu, Z.; Chou, S. Y. Graphene transistors fabricated via transfer-printing in device active-areas on large wafer. *Nano Lett.* **2007**, *7*, 3840–3844.

[18] Reina, A.; Thiele, S.; Jia, X.; Bhaviripudi, S.; Dresselhaus, M.; Schaefer, J.; Kong, J. Growth of large-area single- and bi-layer graphene by controlled carbon precipitation on polycrystalline Ni surfaces. *Nano Res.* **2009**, *2*, 509–516.

[19] Thiele, S.; Reina, A.; Healey, P.; Kedzierski, J.; Wyatt, P.; Hsu, P.; Keast, C.; Schaefer, J.; Kong, J. Engineering polycrystalline Ni films to improve thickness uniformity of the chemical-vapor-deposition-grown graphene films. *Nanotechnology* **2010**, *21*, 015601.

[20] Copel, M.; Reuter, M. C.; Kaxiras, E.; Tromp, R. M. Surfactants in epitaxial growth. *Phys. Rev. Lett.* **1989**, *63*, 632–635.

[21] Li, X.; Cai, W.; Colombo, L.; Ruoff, R. Evolution of graphene growth on Ni and Cu by carbon isotope labeling. *Nano Lett.* **2009**, *9*, 4268–4272.

[22] Zhang, Z.; Duan, Q.; Wang, Z. Micro-mechanisms of fatigure damage in copper crystals. *Acta Metall. Sin.* **2005**, *41*, 1143–1149.

[23] N'Diaye, A. T.; van Gastel, R.; Martinez-Galera, A. J.; Coraux, J.; Hattab, H.; Wall, D.; Meyer zu Heringdorf, F. J.; Horn-von Hoegen, M.; Gomez-Rodriguez, J. M.; Poelsema, B.; Busse, C.; Michely, T. *In situ* observation of stress relaxation in epitaxial graphene. *New J. Phys.* **2009**, *11*, 113056.

[24] Chae, S. J.; Gunes, F.; Kim, K. K.; Kim, E. S.; Han, G. H.; Kim, S. M.; Shin, H. J.; Yoon, S. M.; Choi, J. Y.; Park, M. H.; Yang, C. W.; Pribat, D.; Lee, Y. H. Synthesis of large-area graphene layers on poly-nickel substrate by chemical vapor deposition: Wrinkle formation. *Adv. Mater.* **2009**, *21*, 2328–2333.